Hindawi
Australian Journal of Grape and Wine Research
Volume 2022, Article ID 8121995, 17 pages
https://doi.org/10.1155/2022/8121995

AUSTRALIAN SOCIETY OF VITICULTURE AND OENOLOGY ASVO

Research Article

Spatial and Temporal Trends in the Timing of Budburst for Australian Wine Regions

C. Liles and D. C. Verdon-Kidd

School of Environmental and Life Sciences, College of Engineering, Science and Environment, University of Newcastle, Callaghan, NSW 2308, Australia

Correspondence should be addressed to C. Liles; cindy.liles@uon.edu.au

Received 27 August 2022; Accepted 6 October 2022; Published 30 November 2022

Academic Editor: Justine Vanden Heuvel

Background and Aims. This research investigates spatial and temporal trends in budburst timing across Australian wine regions from 1910–2019. The potential drivers of these observed trends were then identified, including anthropogenic climate change and large-scale climate drivers (El Nino–Southern Oscillation (ENSO), Indian Ocean Dipole (IOD), and Southern Annular Mode (SAM)). *Methods and Results*. The timing of budburst was approximated using accumulation measurements applied to Australia wide gridded temperature data. We show that the modelled budburst date has been gradually shifting to earlier in the year for most (95%) Australian wine regions, at an average rate of one day every 24 years. This linear trend in budburst timing is likely to be associated with steadily increasing air temperatures due to anthropogenic climate change. Significant interannual variability was also observed and was correlated with IOD and SAM; however, no significant relationship was found with ENSO. Positive IOD phases result in budburst occurring on average four days earlier than the long-term average; however, this can be as high as eight days. *Conclusions*. The results of this study highlight that budburst timing for wine grapes is not a stationary phenomenon and is influenced by both natural and anthropogenic conditions. *Significance of the Study*. Understanding variability and trends in modelled budburst timing will assist tactical and strategic management practices and improve phenological modelling and adaptation planning for climate change.

1. Introduction

Wine grapes have an annual developmental cycle known as phenology [1]. Succession through phenological stages is predominately driven by differences in temperature throughout the season [2]. Although the timing and duration of events vary depending on the grape cultivar, climate, and seasonal weather, annual or seasonal variation in climate that departs from the long-term average can alter the timing of phenological stages, which poses a challenge for management at the vineyard scale.

The phenological stage of budburst is the first development event following the winter dormancy period. It is defined by bud formation on the vine, which traditionally occurs in early to mid-spring [1, 3]. The occurrence of budburst is strongly coupled to local air temperature. Therefore, increasing temperatures due to anthropogenic climate change is a recognised threat to this stage in phenological development [4–8]. A long-term variation in budburst timing may lead to growth in unfavourable conditions, resulting in potential changes to vineyard management and may impact wine quality and quantity and, ultimately, a vineyard's long-term viability [8–10].

The potential impacts of changing budburst timing are multilayered. First, an earlier budburst may increase the risk of spring frosts after budburst, which is highly damaging to the vine and will impact the season's crop [11, 12]. Second, since budburst is the first development event, consideration should be given to whether an alteration to budburst timing will have flow-on impacts on the timings of other phenological events such as veraison and overall maturity duration of wine grapes. Several authors have noted advancements in wine grape maturity and the compression of vintages; however, without considering budburst timing, it is uncertain if this is a result of the growing season shortening, shifting earlier, or both [7, 13–16]. Lastly, budburst occurring earlier in the year could result in standard climate accumulation metrics missing an early growth phase. For example, the growing season temperature (GST) is commonly used for wine region classification (i.e., cool climate wines), as well as suitability studies and climate change impact assessments. The GST calculation initiates the temperature summation on 1st October [17–20]. If budburst were to occur significantly earlier than 1st October, then the GST would not capture temperature accumulation for the part of the growing season, and climate classifications may be underrepresented.

To study the historic variability of budburst, a dataset of budburst timing is required. To our knowledge, there is no publicly available long-term record of observed budburst dates for Australian wine regions. Furthermore, phenology data recorded at the vineyard scale introduce complexity around data validity since budburst timing is highly dynamic and influenced by cultivar, maintenance regime, and the grower's definition measurement of budburst. To overcome this, we use a modelling approach to estimate budburst during the study period (1910–2019) across all wine regions. Several authors have developed statistical models (climate metrics) for predicting the budburst date of wine grapes [4, 21–23]. Common to these models is the assumption that initiation of budburst will not begin until an average daily air temperature of between 5°C and 25°C is reached after a winter dormancy period [24–26]. Besides this assumption, there is no globally accepted definition/model for wine grape budburst. However, using heat summation calculations is a common approach applied across the literature [4, 6, 21, 24, 27–31]. Variations in individual temperature accumulation methods occur between the choice of the start date, base temperature (i.e., minimum temperature threshold at which accumulation calculation begins), and temperature threshold defining the budburst event.

In the Australian context, Moncur et al. [23] suggested employing a base temperature of 4°C. This was subsequently adopted in the VineLogic model created by Godwin et al. [21] to predict wine grape phenological development, with applications of the model highlighted by Webb [8]. Recently, Hall et al. [6] have proposed a method using a base temperature of 4.5°C and a threshold of 450°C days of temperature accumulation calculated from 1st July to investigate the budburst date. The study validated the calculation by comparing modelled to observed budburst dates recorded by Coombe and Dry [32]. Hall et al. [6] found that the calculation was reliable in modelling budburst and suggested that using 1st October as a reference budburst date may not represent the Australian climates. Other notable studies include Webb et al. [33], who employed a heat summation formula totalling 8200 hours above a base temperature of 3.7°C calculated from 1st July to indicate budburst for Tasmanian wine regions. Conversely, Jarvis [22] used a GDD calculation with a base value of 10°C starting from 1st September with different thresholds for specific wine cultivars for the 2018 season for vineyards in the Riverina region.

Through the development of a long-term dataset of modelled budburst, timing trends can be identified. In particular, we can determine if budburst timing varies significantly from year to year. This question relates to both the interannual variability in budburst timing and any long-term trends or shifts. On the interannual scale, Australia's climate is influenced by a range of oceanic-atmospheric climate modes [34]. The three major climate drivers that influence the continent are the El Niño/Southern Oscillation (ENSO), Indian Ocean Dipole (IOD), and Southern Annular Mode (SAM), as summarised in Table 1.

In Australia, Jarvis et al. [29, 39] have conducted several studies investigating the influence of climate drivers on wine regions [39, 40]. Their analysis showed that ENSO and IOD influence wine grape maturity, with the IOD being most influential for eastern wine regions. This research included a springtime temperature parameter (summed maximum daily temperature); however, this was assessed through the lens of timing for wine grape maturity rather than budburst. Furthermore, the potential impact of SAM was not addressed. Therefore, the influence of Australia's climate drivers, specifically on budburst timing, remains a significant knowledge gap.

Compounding interannual climate variability is the impact of anthropogenic climate change, which manifests in a long-term increasing trend in air temperature (crucial for budburst). Climate change impacts have already been observed, with Australia's climate warming by 0.9°C since 1910 [34]. Springtime temperatures (when budburst occurs) are increasing more rapidly than temperatures during other times of the year [41]. There is evidence that increasing temperatures are being experienced across Australian wine regions [13, 14, 16]. However, to date, there has not been an Australia wide study of the impact of such temperature trends on the timing of budburst.

This paper aims to investigate variability in the timing of budburst across Australian wine regions (since 1910) and assess any temporal trends and their causes. To date, this has been the first paper to investigate the combined spatial and temporal variability of wine grape budburst. By characterising trends in budburst timing and identifying climatic influences, these findings can help inform tactical and strategic vineyard management practices and future planning to promote the continuation of the renowned Australian wine industry.

2. Materials and Methods

2.1. Study Area. Australia's diverse climate and elevation enable vineyards to grow over 146 grape varieties ranging from cool climate to hot climate wines [42, 43]. Shiraz, Cabernet Sauvignon, and Chardonnay are the most popular wine cultivars accounting for over 60% of the 2021 total crush [44]. This study reviews spatial and temporal trends relevant to the Shiraz wine grape, known to have an early to midseason budburst.

Table 1: Climate drivers that influence Australian climate.

Climate drivers	Brief description and impact on Australian climate	Spatial influence (within Australia)
El Nino–Southern Oscillation (ENSO)	ENSO events are driven by changes in the ocean and atmospheric conditions of the equatorial Pacific Ocean. The El Nino (ENSO positive) phase tends to be associated with warm and dry weather, while the opposite occurs during the La Nina phase [35]	Primarily eastern and Northern Australia
Indian Ocean Dipole (IOD)	IOD events are driven by a sea surface temperature gradient in the tropical Indian Ocean, where an IOD positive is associated with warm and dry weather (while the reverse tends to occur during IOD negative) [36]	Most of Australia, particularly southeast
Southern Annular Mode (SAM)	SAM is defined by changes in westerly winds driven by temperature contrasts between the tropics and southern polar regions. In the positive phase, these conditions inhibit Antarctic air outbreaks moving north and influencing temperature, whereas in the negative mode, Antarctic air to spill north more easily [37, 38]	Primarily Southern Australia

The Wine Australia Geographic Indicators (GIs) identify unique wine regions within Australia and were used to define the study area, as shown in Figure 1. The study area has approximate longitude limits of 135.7° to 153.7°and approximate latitude limits of −39.5° to −23.6°, covering an area of 2 262 508 km^2.

2.2. Data. Gridded daily minimum and maximum temperature data at 5 km resolution from 1910 to 2019 were sourced from the Bureau of Meteorology (BOM). The average daily temperature (required for the modelled budburst date analysis) was generated from the daily maximum and minimum values.

Indices representing the large-scale climate modes (ENSO and IOD) were obtained from the KNMI explorer (https://climexp.knmi.nl/start.cgi), while the SAM index was obtained from the NOAA Physical Sciences Laboratory (https://psl.noaa.gov/data/20thC_Rean/timeseries/monthly/SAM/). The index value for each year was extracted for the average of July, August, and September (three months leading up to typical budburst in the Southern Hemisphere). Data were extracted for 1910–2019 for ENSO and IOD and 1910–2012 for SAM (note this is due to the limitations of the index availability post 1912).

For the IOD, in addition to the Dipole Mode Index (DMI), the individual poles of the dipole (Eastern Pole and Western Pole) were also investigated, as previous research highlighted that these regions often have a stronger teleconnection to the Australian climate than the dipole itself [36]. Table 2 provides more details of the index (indices) representing each climate driver, while Figure 2 illustrates each climate driver's climate phase (positive and negative) during the study period. The individual poles of the IOD display a positive trend, consistent with the well-documented warming of the Indian Ocean [47].

3. Methods

By following the method of Hall et al. [6], the budburst date was calculated using a growing degree day (GDD) equation with a base temperature of 4.5°C (GDD4.5). The modelled budburst date is calculated as the number of days after 1st July on which accumulated daily GDD4.5 reaches 450 days °C. The output from this calculation represents the number of days after 1st July on which budburst theoretically occurred; for example, 31 represents 1st August. This calculation has been developed for Shiraz wine grapes. The modelled budburst date (herein referred to as a "budburst date") was calculated for the entire Australian grid using *Python* coding software from 1910 to 2019.

The method proposed by Hall et al. [6] was chosen because of its recent development and relevance to Australian conditions. As highlighted in the Introduction, Hall et al. [6] also validated their metric against observed budburst dates from vineyard phenological records. To ensure consistency within our study, we compared our modelled budburst dates to observed/recorded dates presented in the literature for 58 vineyards and/or years. We found the methodology of the modelled budburst date of Hall et al. [6] to be comparable to the existing literature, including observed records.

Spatial statistics within ESRI ArcGIS were used to determine budburst statistics including the spatial median, minimum, maximum, and majority budburst dates for each wine region. Zonal statistics were used to determine the median budburst dates across the wine regions.

A time series analysis of yearly budburst dates was conducted to assess both linear and nonlinear trends at a wine region level. Two nonparametric tests were used: (1) Mann–Kendal test to determine significant linear trends in the time series and (2) distribution-free cumulative sum (CUSUM) to test if the mean is statistically different across two time periods to determine step changes in the data over time. TREND software [48] and the Mann–Kendall package developed for *Python* software [49] were used for processing the analysis.

Budburst dates were grouped into positive and negative phases of each climate driver (ENSO, IOD, and SAM) to assess potential associations between budburst date and climate drivers. A positive (negative) phase was defined as climate index values > 0.5 (<−0.5) standard deviations from the mean [36]. Student's *t*-tests were applied to assess the statistical significance of observed differences in the means of climate groupings, whereby:

(i) If a p value is≥0.05, the difference in the mean between the two datasets is not significant

(ii) If a p value ≤0.05, the difference in the mean between the two datasets is significant

Lastly, to assess the magnitude of influence of large-scale climate drivers, the mean budburst date for each climate phase (positive/negative) was calculated for each wine region and each climate driver. Box plots of budburst dates per phase (including neutral phases) were also generated to visually illustrate the magnitude of climate drivers' influence on selected wine regions.

SciPy and Seaborn *Python* software packages were used to undertake statistical analysis and visualisation in relation to interannual variability [50, 51].

4. Results

4.1. Spatial Variability of Budburst Timing across Australian Wine Regions. The spatial variability in the timing of modelled budburst dates within Australian wine regions was first assessed. It was found that the majority of Australian wine regions have the median budburst date during September (calculated over 1910–2019) (Figure 3(a)). However, this can be as early as mid-to-late August for the South Burnett, Hastings River, Margaret River, and Swan District wine regions. For regions at higher elevation, the budburst date extends into October. The cool climate Tasmanian wine region has the latest budburst date of all regions, where budburst tends to occur in November, including some areas that do not reach the budburst temperature accumulation threshold before the end of the year.

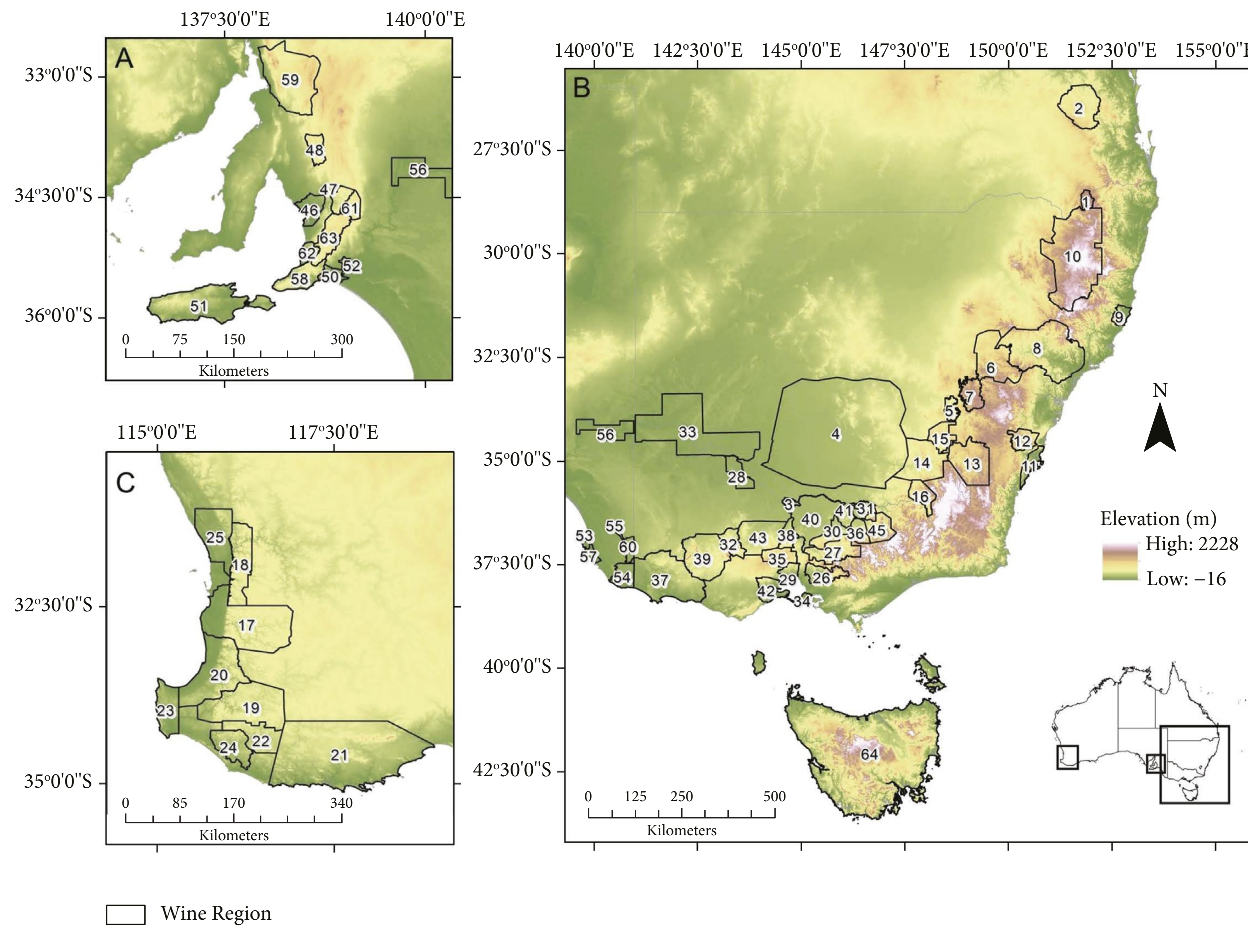

ID	Wine Region	ID	Wine Region	ID	Wine Region	ID	Wine Region
1	Granite Belt	17	Peel	33	Murray Darling	49	Coonawarra
2	South Burnett	18	Perth Hills	34	Mornington Peninsula	50	Currency Creek
3	Perricoota	19	Blackwood Valley	35	Macedon Ranges	51	Kangaroo Island
4	Riverina	20	Geographe	36	King Valley	52	Langhorne Creek
5	Cowra	21	Great Southern	37	Henty	53	Mount Benson
6	Mudgee	22	Manjimup	38	Heathcote	54	Mount Gambier
7	Orange	23	Margaret River	39	Grampians	55	Padthaway
8	Hunter	24	Pemberton	40	Goulburn Valley	56	Riverland
9	Hastings River	25	Swan District	41	Glenrowan	57	Robe
10	New England Australia	26	Yarra Valley	42	Geelong	58	Southern Fleurieu
11	Shoalhaven Coast	27	Upper Goulburn	43	Bendigo	59	Southern Flinders Ranges
12	Southern Highlands	28	Swan Hill	44	Beechworth	60	Wrattonbully
13	Canberra District	29	Sunbury	45	Alpine Valleys	61	Eden Valley
14	Gundagai	30	Strathbogie Ranges	46	Adelaide Plains	62	McLaren Vale
15	Hilltops	31	Rutherglen	47	Barossa Valley	63	Adelaide Hills
16	Tumbarumba	32	Pyrenees	48	Clare Valley	64	Tasmania

FIGURE 1: Location and elevation of the 64 established Australian wine regions (elevation data obtained from Geoscience Australia [43]. (A) South Australia, (B) eastern Australia, and (C) Western Australia.

The minimum (i.e., earliest) and maximum (i.e., latest) budburst dates across the study region are shown in Figures 3(b) and 3(c). The results confirm that no wine regions have experienced budburst prior to August (based on our metrics). The regions that experience the earliest budburst date (August) are South Burnett, Hunter, Hastings River, Shoalhaven Coast, Peel, Perth Hills, Geographe, Great Southern, Margaret River, Pemberton, Swan District,

Table 2: Climatic indices used in this study.

Climate drivers	Dataset
ENSO	Nino 3.4: monthly version of HadISST sea surface temperature, averaging anomalies over region lon = −170–120, lat = −5–5° [45]
Eastern pole of the IOD (IOD-E)	SEIO: monthly version of NOAA ERSSTv5, averaging anomalies over region lon = 89–111, lat = −11–1° [46]
Western pole of the IOD (IOD-W)	WTIO: monthly version of NOAA ERSSTv5, averaging anomalies over region lon = 49–71, lat = −11–11°, [46]
IOD	DMI: Difference between IOD-E and IOD-W [46]
SAM	Represented by the Antarctic Oscillation (AAO): defined as the leading principal component (PC) of 850 hPa geopotential height anomalies south of 20S (Thompson and Wallace 2000)

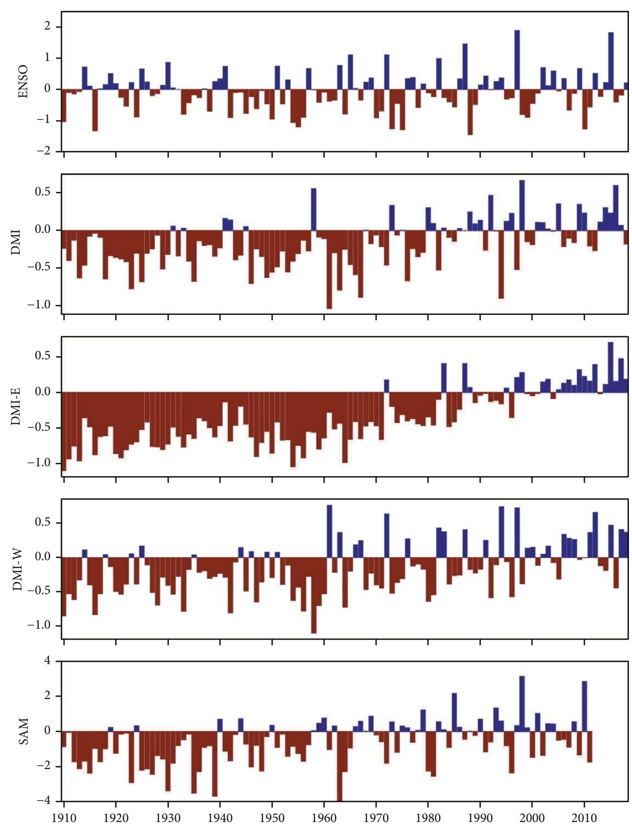

Figure 2: Time series of averaged July, August, and September climate indices for ENSO, DMI, DMI-E, DMI-W (1910–2019), and SAM (1910–2012). Dark blue indicates that the index is positive. Dark red indicates that the index is negative.

Kangaroo Island, and Southern Flinders Ranges. Regions with a minimum budburst date within early October include Orange, Canberra District, Hilltops, Tumbarumba, Upper Goulburn, Strathbogie Ranges, Macedon Ranges, King Valley, Beechworth, and Alpine Valleys. All other wine regions (including Tasmania) have a minimum date in September and are located at higher elevations. Maximum budburst dates are more varied than other statistics (Figure 3(c)). For example, the latest budburst date that occurs for the Margaret River and Swan District is mid-to-late August, while budburst can occur as late as December for Canberra District, Yarra Valley, Upper Goulburn, Grampians, Alpine Valleys, and Tasmania. Again, wine regions located at higher elevations experience later budburst dates.

The median zonal statistics were calculated to identify the budburst date across each wine region (Figure 3(d)). Results show that a typical wine region in Australia would experience budburst in late September (25th September). The minimum and maximum budburst occur on 14th September and 16th October, respectively.

Figure 4 highlights the historical range (over the 110-year period) in budburst timing for each wine region (organised in ascending order of the median budburst date). The variability in budburst timing for individual wine regions is considerable, with the majority of wine regions exhibiting a range of six weeks between the historical minimum and maximum budburst date. Wine regions that experience a lower degree of variability (less than a week

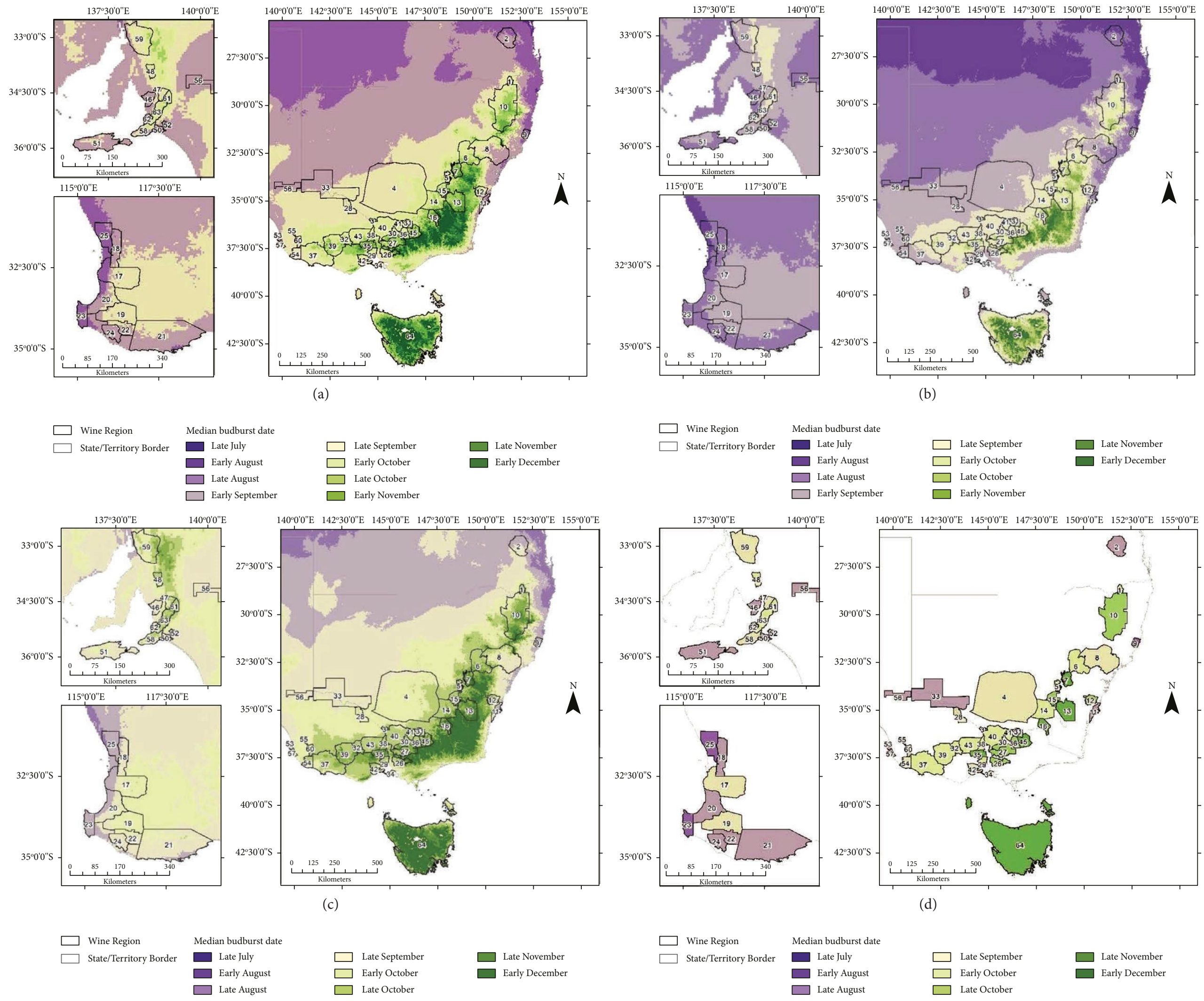

FIGURE 3: Summary statistics of modelled budburst timing across Australian wine regions between 1910 and 2019(a) median, (b) minimum, (c) maximum (d) zonal median across wine regions.

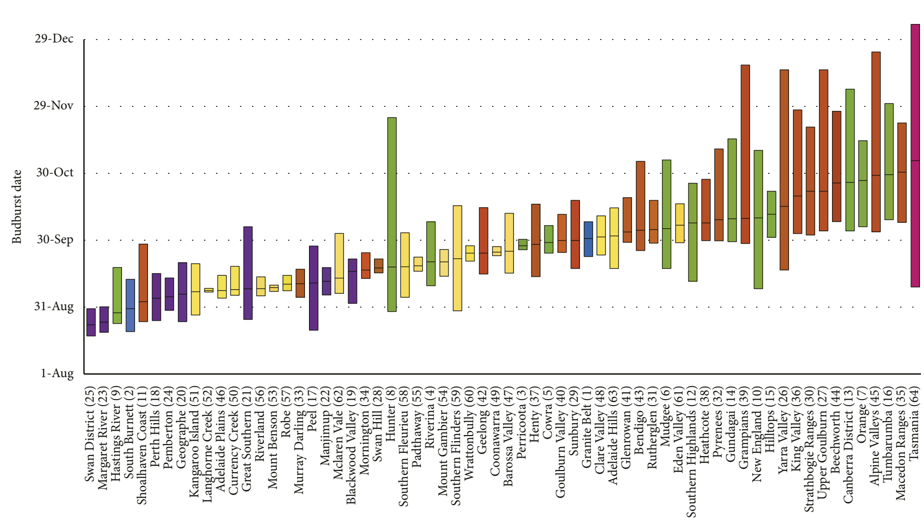

FIGURE 4: -Distribution of modelled budburst dates for Australian wine regions between 1910 and 2019, in ascending order by mean date, showing Queensland (purple), New South Wales (green), Victoria (orange), South Australia (yellow), and Tasmania (pink).

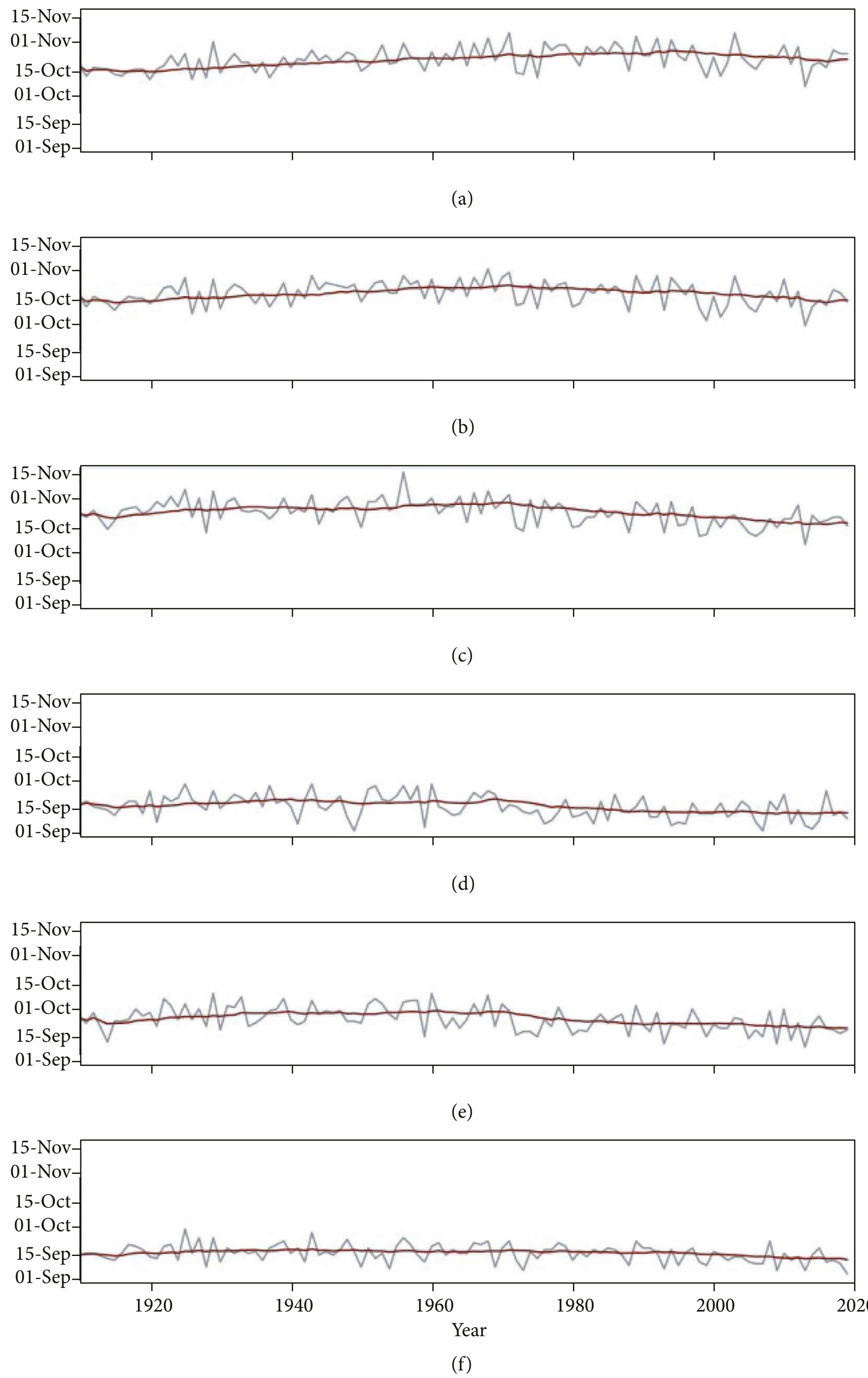

Figure 5: Time series maps (1910–2019) for selected wine regions showing the yearly median modelled budburst date (grey line) and the 20-year moving average trend (dark red line): (a) Beechworth, (b) Upper Goulburn, (c) Canberra, (d) Peel, (e) Barossa, and (f) Hunter wine region.

between the historical range) include Langhorne Creek, Mount Benson, Coonawarra, Perricoota, Padthaway, Swan Hill, Wrattonbully, and Robe. Tasmania has the largest range in budburst dates, with 16 weeks between the minimum and maximum. However, it is noted that the Tasmanian wine region covers the entire state, and therefore, a higher range is expected due to the large geographic domain. Indeed, these results should be considered alongside the variability in the geography of wine regions (i.e., size, topography, and aspect). For example, the Riverina GI wine region covers 78,000 km^2, and as such, it is expected to have a larger variation in geography than smaller scaled wine regions.

Table 3: Trend analysis of Australia wide average time series (1910–2019) of modelled budburst dates.

Modelled budburst statistic	Statistic test	Result	Interpretation
Minimum	Mann–Kendall	p (0.01)	Decreasing trend
	CUSUM	p (0.05) year change = 1978	Data in earlier years are higher than in later years
Maximum	Mann–Kendall	p (0.01)	Decreasing trend
	CUSUM	p (0.01) year change = 1978	Data in earlier years are higher than in later years
Median	Mann–Kendall	p (0.01)	Decreasing trend
	CUSUM	p (0.05) year change = 1978	Data in earlier years are higher than in later years

Other regions with a large range (more than 6 weeks) include Yarra Valley, Hunter, Alpine Valleys, Grampians, Upper Goulburn, Canberra District, New England Australia, King Valley, Tumbarumba, and Beechworth.

Overall, the spatial variability observed is consistent with the known climate of the wine regions. For example, regions that are known to experience warmer conditions, such as Swan District, Hunter Valley, or Riverland, have been identified to be experiencing budburst earlier in the season compared to regions with cooler climate conditions, such as Yarra Valley, Canberra, and Orange. However, it is also clear (from the range in dates for individual wine regions) that each region has experienced considerable temporal variability in budburst timing. This will be further explored in Section 4.2.

4.2. Temporal Variability of Budburst Timing for Australian Wine Regions. To analyse temporal trends in the timing of modelled budburst dates between 1910 and 2019, a subset of representative wine regions was initially chosen to apply trend statistics using the median budburst date across the wine region. Wine regions were selected, taking into consideration location and topography. The time series graphs are shown in Figure 5 with (A) Beechworth, (B) Upper Goulburn, (C) Canberra, (D) Peel, (E) Barossa, and (F) Hunter.

The time series of budburst dates for Canberra (Figure 5(c)), Peel (Figure 5(d)), and Barossa (Figure 5(e)) displays a clear advancement in budburst dates (occurring earlier) for the recent period, whereas budburst dates for Beechworth (Figure 5(a)), Upper Goulburn (Figure 5(b)), and Hunter (Figure 5(f)) appear more stable throughout 120 years (i.e., no obvious linear trends). Interestingly, budburst timing at Beechworth (Figure 5(a)) during the most recent 20 years appears similar to conditions from the beginning of the twentieth century (both periods display early budburst timing at this location). Furthermore, all regions show a high degree of year-to-year variability in the timing of budburst, which is explored further in Section 3.

To further investigate these apparent trends, the Mann–Kendall and CUSUM tests were applied to the minimum, maximum, and median budburst date time series data. As an initial assessment, individual wine region dates were collated into a single averaged time series of minimum, maximum, and medium budburst dates for each year to test for general trends across the collective regions (Table 3). All three statistics (minimum, maximum, and median budburst) exhibit a statistically significant decreasing trend according to the Mann–Kendall test, highlighting that the budburst date has been occurring earlier in the year in recent decades. Furthermore, the CUSUM test identified a step change in the time series data in 1978, with budburst occurring earlier in the season after this year. The step change for maximum budburst showed the strongest statistical significance ($p = 0.01$) compared to other datasets.

Temporal trends of budburst dates for each wine region were then subsequently analysed to determine if the changes observed in Table 4 and Figure 5 occur across the majority of wine regions, or if these trends are dominated by particular regions. In this case, the Mann–Kendall statistic was used to determine the direction (i.e., increasing or decreasing) of the trend for the median budburst dates within each wine region over the study period (Figure 6). The results confirm that the budburst date has advanced in recent decades for the majority of wine regions. However, some wine regions show no trend in the budburst date, including Alpine Valleys, Bendigo, Clare Valley, Cowra, Goulburn Valley, Gundagai, Heathcote, Hilltops, Mudgee, Padthaway, Perricoota, Pyrenees, Riverina, Rutherglen, Southern Flinders Ranges, Strathbogie Ranges, Swan Hill, Upper Goulburn, and Wrattonbully. The majority of these wine regions share the characteristics of being cool climate wine regions and are located at higher elevation, with the exception of the Riverina wine region. Three wine regions, Glenrowan, Beechworth, and King Valley, display an increasing trend, indicating that budburst for these regions has been occurring later in the year in recent decades. Interestingly, these wine regions are also cool climates and at higher elevations.

The Theil–Sen Slope of the Mann–Kendall statistic was calculated to quantify the rate of change (days/years) in budburst timing experienced across the wine regions between 1910 and 2019 (rates for each wine region are included in Supplementary Table 1). The rates of change are between −0.11 days per year at Adelaide Hills and 0.74 days per year at Beechworth. The average rate of change in modelled budburst dates across Australian wine regions is −0.04 days per year. This equates to the budburst shifting one day earlier every 24 years. However, this could be as quick as one day every nine (9) years, as seen at Adelaide Hills.

4.3. Impact of Large-Scale Climate Drivers on Budburst Timing. To investigate potential relationships between large-scale climate models and budburst timing, modelled budburst dates were grouped according to the climate phase (positive or negative) and Student's t-test was applied. The results are summarised spatially in Figure 7. Additionally,

Table 4: Change in minimum, maximum, and average modelled budburst between positive and negative climate phases, calculated between 1910 and 2019

	Δ mean	ENSO	IOD	IOD-E	IOD-W	SAM
All wine regions	Min	−2.64	−8.15	−8.54	−6.26	−5.00
	Max	1.78	0.67	4.38	3.14	3.30
	Average	−0.34	−3.44	−2.06	−1.87	−0.42
Only wine regions with t-test p value <0.05	Min	—	−8.15	−8.54	−6.26	−5.00
	Max	—	−2.79	−3.38	3.14	3.30
	Average	—	−4.73	−5.33	−3.77	−2.22

*A negative value indicates that budburst occurs earlier during the positive phase of the respective climate driver.

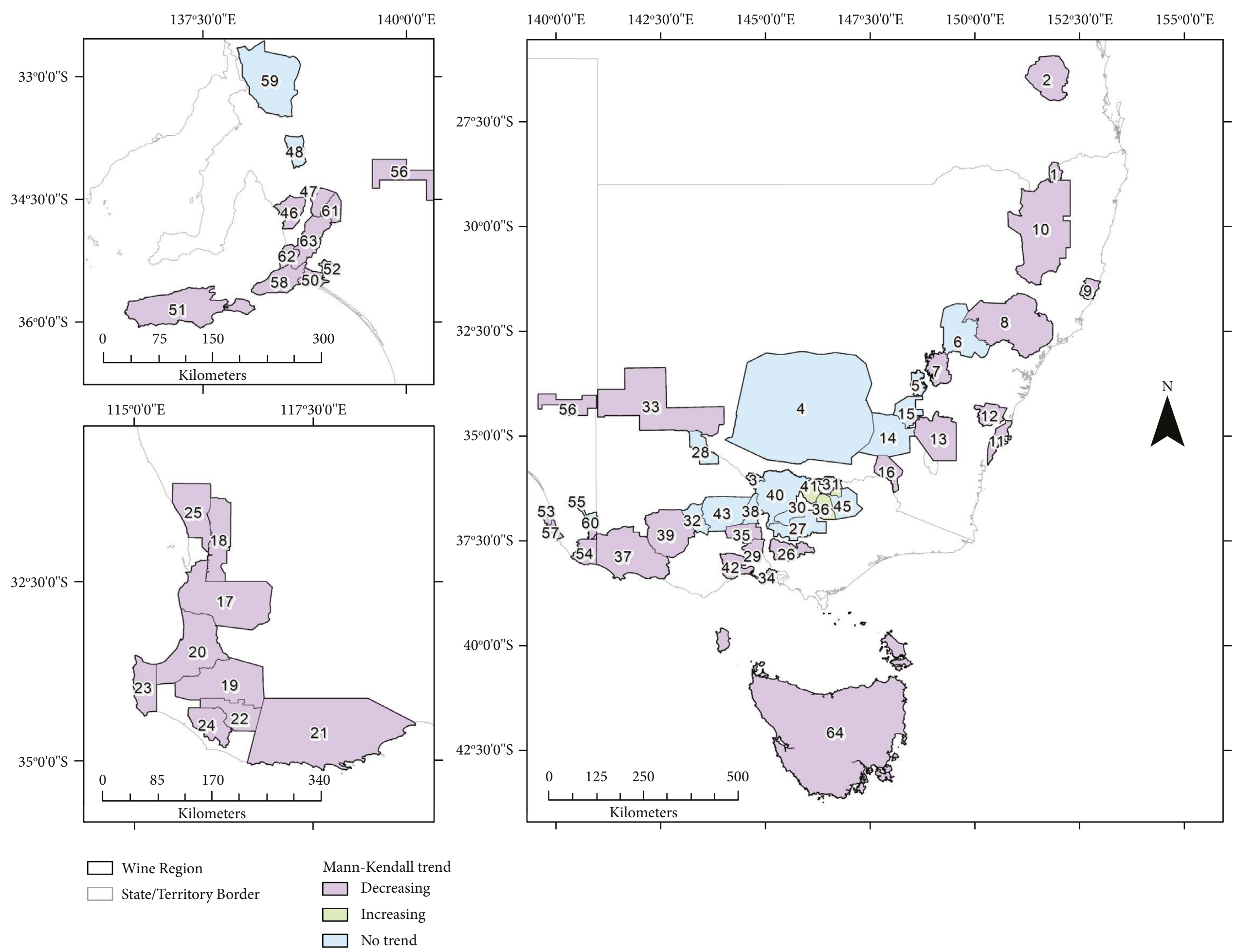

Figure 6: Mann–Kendall trend of modelled budburst timing between 1910 and 2019.

individual wine region results are included in Supplementary Table 2. To quantify the magnitude of the change in date, the mean budburst date for each climate phase was calculated for each wine region and climate driver. The difference in the mean budburst date between different phases is shown in Supplementary Table 3 and summarised in Table 4.

A statistically significant difference in the mean budburst date between positive and negative phases of the climate modes was identified for almost three-quarters (72%) of the wine regions. IOD and SAM had the greatest impact on budburst timing of three climate drivers, while no significant relationship was identified with ENSO phases.

The IOD has been shown to influence most wine regions (55%), as shown in Figure 7(b). The geographic impact is substantial, influencing wine regions across eastern Australia, including South Australian wine regions, as well as Pemberton and Great Southern wine regions located in Western Australia. Results highlight that during the positive IOD phase, budburst occurs 4.7 days earlier on average. Of different IOD indices, IOD-E has the largest influence on budburst causing budburst to occur on average 5.3 days earlier under positive conditions (i.e., warm SSTs in the northeast Australian region); however, it could be as high as 8.5 days (seen in the Granite Belt). IOD-E modulates 20% of

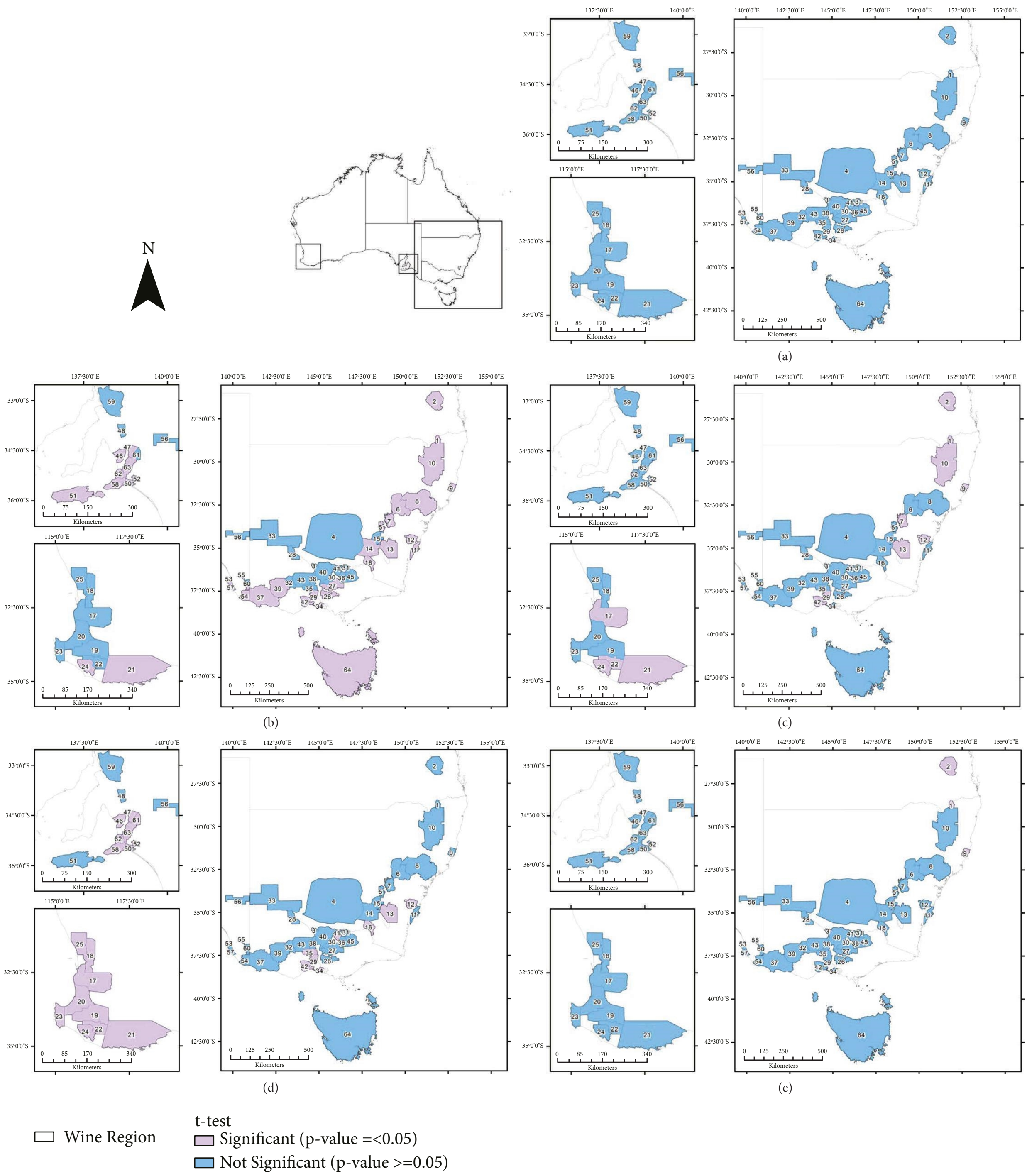

Figure 7: *t*-test statistic between the climate index and the modelled budburst date for (a) ENSO, (b) IOD, (c) IOD-E, (d) IOD-W, and (e) SAM.

wine regions, with a diverse geographic influence, as shown in Figure 7(c).

Furthermore, 39% of wine regions are influenced by the IOD-W climate driver, as shown in Figure 7(d). When SSTs are warmer than usual in this region, the budburst date shifts 3.8 days earlier on average. All Western Australian wine regions are influenced by IOD-W. The SAM was also identified as a significant influence on a small number of wine regions, including Granite Belt, Hastings River, South Burnett, and Perricoota. A positive phase of the SAM in this case results in the budburst date shifting 2.2 days earlier on average.

To observe the full range (rather than just the median) of the budburst date that has occurred within the different phases of each climate mode, a selection of representative wine regions was chosen, and boxplots of budburst dates were constructed according to each climate phase (i.e.,

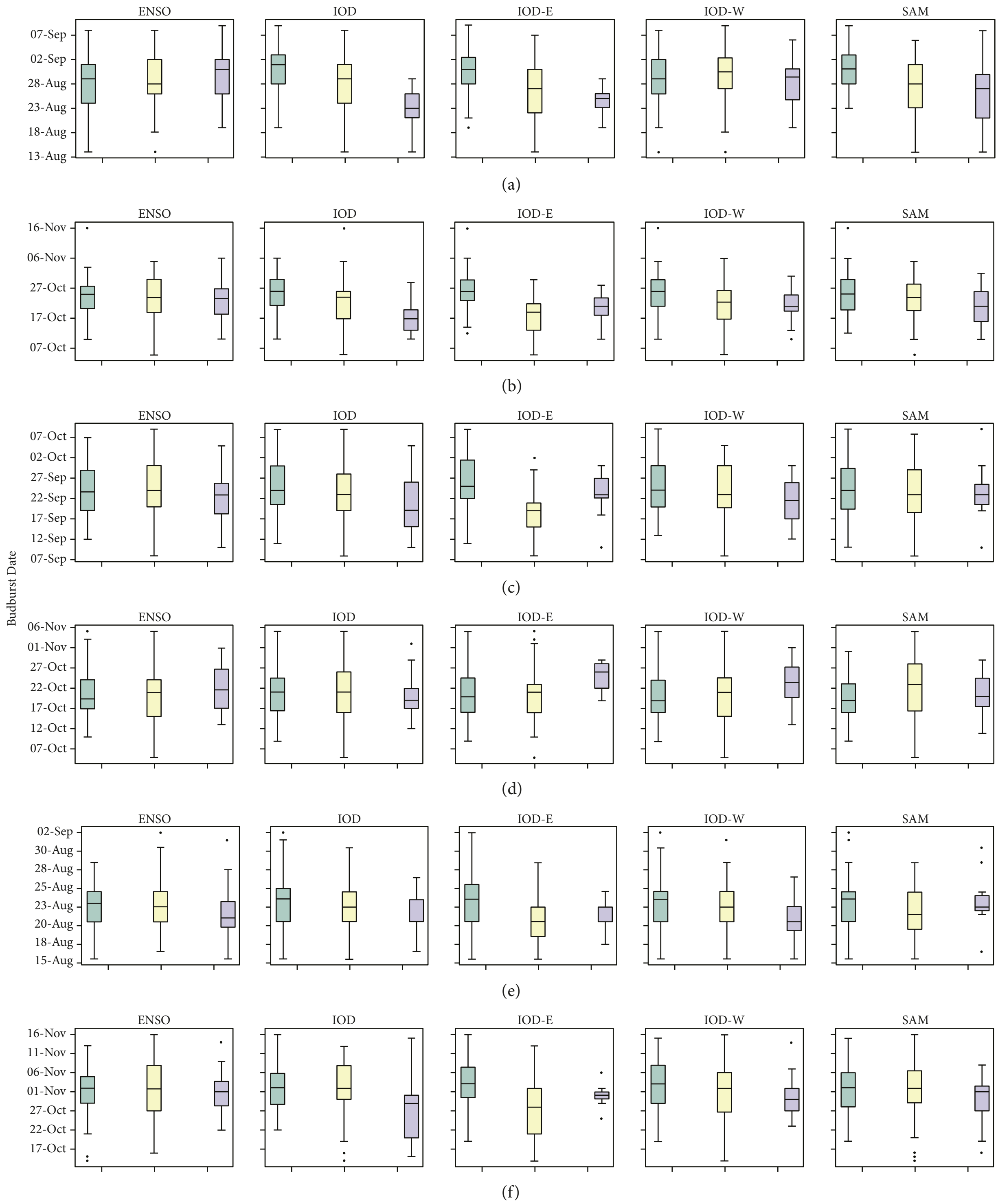

Figure 8: Box plots of modelled budburst dates stratified according to negative (green), neutral (yellow), and positive (purple) of the climate drivers for wine regions: (a) South Burnett, (b) Canberra, (c) Barossa Valley, (d) Beechworth, (e) Margaret River, and (f) Tasmania.

positive, neutral, and negative, Figure 8). The example wine regions were chosen to take into consideration location, topography, and *t*-test results:

(a) South Burnett: a north-eastern wine region that demonstrated an association with IOD, IOD-E and SAM

(b) Canberra: a central NSW region that demonstrated association with all IOD indices

(c) Barossa: a significant South Australian wine region that demonstrated an association with IOD and IOD-W,

(d) Beechworth: a central Victoria wine region that demonstrated an increasing temporal trend and no association with climate drivers

(e) Margaret River: a significant Western Australian wine region that demonstrated an association with IOD-W

(f) Tasmania: a southern wine region that demonstrated an association with the IOD

The box plots confirm the influence of the climate drivers on the distribution of historical budburst dates. This is quite compelling for some locations. For example, in the South Burnett (Figure 8(a)), the interquartile range (i.e., 50% of the data) of budburst timing does not overlap between the positive and negative phases of IOD or IOD-E. This highlights the particularly strong influence of climate drivers on this wine region. Additionally, the South Burnett was also shown to be influenced by SAM, while the interquartile ranges of the positive and negative phases are unique (suggesting an association), and it is noted that the positive and neutral phases share a similar range, with the negative phase showing a higher (later) range of budburst. A strong influence by the IOD is observed in Figure 8(b) for the Canberra wine region, with budburst date distributions being distinct between positive and negative phases of the IOD. Consistent with the t -test analysis, the box plots do not suggest a relationship between ENSO and budburst.

There are some unexpected results when observing the box plots, such as the Barossa Valley (Figure 8(c)), which shows an overlap of the interquartile range of both the positive and negative phases; however, the neutral phase demonstrates a lower (earlier) budburst date. Furthermore, Beechworth (Figure 8(d)) did not demonstrate an association with any climate drivers using the t –test; however, the boxplot for IOD-E displayed a small range of budburst during the positive phase compared to a much large range for both the negative and neutral phases (i.e., budburst is more variable during IOD-E negative for this region). These results indicate there may be subtle impacts that warrant further investigation of climate driver influence at the wine region scale or even the vineyard scale.

5. Discussion

This study aimed to assess the spatial variability in the timing of budburst for wine grapes across Australian wine regions and investigate long-term trends and interannual variability. To achieve this, we calculated a theoretical (modelled) budburst date for each year (1910–2019) using a GDD calculation with a base of 4.5°C and a threshold of 450 as proposed by Moncur, Rattigan et al. [23] and recently validated by Hall, Mathews et al. [6]. This was applied to spatially gridded temperature data that covered all Australian wine regions. The spatial analysis demonstrated that the timing of budburst dates varies significantly across Australian wine regions. Results show that budburst is expected to occur in September (with an overall median date of 25th September). However, some regions experience the budburst in late August, whereas for regions at elevation, this can extend into October. Indeed, elevation appeared to be the main driver in the spatial patterns observed. It was also noted that regions with low elevation, but a cool climate, experienced an earlier budburst date than regions with higher elevation and an intermediate/warm climate wine classification.

Temporal analysis was conducted to determine trends in budburst timing, namely, determining the gradual linear trends associated with the impacts of anthropogenic climate change and interannual variability associated with climate drivers. A time series analysis confirmed that the budburst date has been occurring earlier in the year (since 1978) for the vast majority of wine regions. However, the Mann–Kendall analysis also identified an increasing or no trend in a budburst date for a small number of wine regions. This may be due to the start of the record (1910–1920) corresponding to a very warm and dry period of the Australian climate (which advanced budburst for at least some regions during this time (e.g., Beechworth).

The Theil–Sen Slope results estimated that the budburst date progressively occurs on average one day earlier every 24 years; however, this could be as quick as one day every nine years for some wine regions. This continued shift to earlier budburst timing coincides with the well-established trend in air temperatures associated with anthropogenic climate change. Indeed, Australian air temperatures have warmed by 1.4°C since 1910, and since 1950, every decade has been warmer than the decade prior [34]. This study considers the rate of change over the entire time period (1910–2019); however, given the accelerated temperature increases in the last 20 years, it would be hypothesised that the advancement of the budburst would be more pronounced in the twenty-first century.

In this study, we have focused on historical trends in budburst timing over the instrumental period; however, further research should be conducted to quantify changes to budburst dates under future climate change scenarios. Research has shown that the global surface temperature will continue to increase regardless of which future emission scenario eventuates, with best estimates showing the increase between 1.5°C and 4.4°C by 2100 [52]. Due to the projected acceleration of temperatures, future changes in budburst timing may be more dramatic, which could result in an increased risk of dual warming as budburst shifts earlier in the season while advancing to grape maturity timing, as suggested by Jarvis, Barlow et al. [39] and Webb, Whetton et al. [8].

A temporal analysis was also conducted to determine the influence of large-scale climate drivers on interannual variability in budburst dates. This was investigated by grouping budburst dates into the three phases of each climate driver (positive, negative, and neutral) due to previous studies highlighting the frequent nonlinear impacts of drivers on the Australian climate [53]. Using Student's t-test, a statistically significant relationship was observed between the budburst date time series and the indices of climate drivers for 46 wine regions in Australia (72% of wine regions). Somewhat surprising (due to the well-known influence of ENSO on the Australian climate), the ENSO was not shown to have a significant association with budburst timing for Australian wine regions. However, this is likely due to the very specific timing of budburst during spring. As noted by Jones and Trewin [35], the ENSO has a much smaller impact on cool season temperatures than on warm season temperatures. Furthermore, the ENSO tends to impact the diurnal range more than the average temperature (which is the metric used here for budburst). As such, although the ENSO may not be the main driver of budburst timing, it may influence the timing of other phenological stages in warmer months; for example, Jarvis, Darbyshire et al. [29] showed that the ENSO can impact wine grape maturity timing.

Of all the three climate modes studied here, the IOD exhibited the most widespread influence, resulting in a significant impact on budburst timing for wine regions located on the northeast coast and SA, as well as a few regions in WA. The individual poles of the IOD (IOD-E and IOD-W) also showed an association with budburst, with IOD-E demonstrating the strongest relationship. The findings presented here are consistent with those in previous studies that have highlighted that the IOD has the most influence of large-scale drivers on Australian air temperature during winter and springtime [14, 54–56].

The SAM was shown to significantly influence budburst timing for wine regions located at Granite Belt, Hastings River, South Burnett, and Perricoota. Previous research has identified that the positive phase of the SAM during cooler months is typically associated with drier and cooler conditions over the southwest and southeast coast [38, 55]. However, the wine regions with significant SAM impacts on budburst identified in this paper are not spatially consistent, suggesting that there may be other modes masking the influence of the SAM (such as the IOD and ENSO). Further research is required to assess multimodel impacts (i.e., drivers acting in combination) on budburst dates. This may also assist in untangling ENSO impacts that may not be observable in isolation.

Several wine regions showed no influence (in terms of budburst dates) by any of climate drivers including, Alpine Valleys, Beechworth, Bendigo, Clare Valley, Goulburn Valley, Heathcote, Hilltops, King Valley, Murray Darling, Padthaway, Pyrenees, Riverina, Riverland, Rutherglen, Southern Flinders Ranges, Strathbogie Ranges, Swan Hill, and Wrattonbully. These wine regions share characteristics of being inland wine regions with lower interannual variability in their budburst date. As such, these regions are more highly influenced by the long-term temperature increase rather than interannual climate modes.

This study focused purely on the average air temperature in the accumulation metric to model budburst timing since this has been identified as the most influential parameter [28]. However, other studies have also suggested that maximum temperatures may influence early season phenological events such as budburst, even more than temperature accumulation [4]. Beyond temperature, there are other influences such as winter dormancy or sunlight hours and nonclimate influences, such as management techniques, which can advance or delay budburst [27, 57]. These metrics could also be considered in future research, particularly in developing adaptation plans to combat changes in the timing of various phenological stages of wine grapes.

It is acknowledged that the primary limitation of this study is the theoretical calculation of budburst that may not align with actual budburst occurrence at the vineyard scale. However, in the absence of long-term observational datasets, the modelled dataset represents a reasonable approach to study variability in the budburst date, allowing for long-term trends to be assessed. It is recommended that these findings should be used to inform vineyard scale practices; further refinements would be required, taking into account the observed budburst. Nonetheless, through understanding the potential impact of climate influences, tactical and or strategic planning can be conducted; e.g., weather forecasting may identify positive IOD influences coming into spring, allowing vineyards to consider the potential of earlier budburst. A further limitation of our study is that the accumulation threshold applied here was derived primarily for Shiraz, and different cultivars may display varying sensitivities to temperature accumulation. As such, the thresholds would need to be defined at the vineyard scale and for each cultivar in order to use this as a guide for individual vineyard management practices. Nonetheless, in this research, we focus purely on trends and identification of influences at the wine region scale, which are likely to be insightful for a range of cultivars.

Overall, there are a number of management implications arising from the results of this study. First, budburst occurring earlier in the year may pose an additional risk from frost postbudburst. El Nino is associated with a decreased cloud cover that often leads to cooler than average night time temperatures during winter–spring, leading to 15–30% more frost days, particularly across eastern Australia [58]. Therefore, although the ENSO may not be the main driver of budburst timing, the combination of IOD positive and El Nino could pose a significant risk of early budburst and increased frost risk.

Second, this research has demonstrated that budburst may occur in September, which has implications for the accuracy of phenological models, which typically use 1st October to describe the beginning of the growing season and may not capture an early phase of growth under a changing and variable climate. For example, extrapolating the trend in budburst advancement at a similar rate to the last ~40 years (i.e., no further acceleration), budburst by 2100 for a typical wine region could occur in early September, and regions currently experiencing earlier budburst may experience budburst in mid-August. It is recommended that future research should identify potential changes to budburst timing as well as other phenological stages under future climate change projections to quantify and assess impacts. Third, numerous studies have found advancement in maturity and harvest dates, which are measured as days from budburst [7, 14, 16]. Considering this research, it is found that the budburst date is occurring earlier, and questions are raised about whether the maturity is also occurring earlier or if the season is shifting. Further research should be conducted to consider the whole-of-life phenological cycle. Finally, although we have focused on the large-scale, Australian context, this work is relevant for other global wine regions where relationships have also been identified between local climatic drivers and wine grape phenology.

6. Conclusion

This study improves our understanding of budburst timing for wine grapes across Australian wine regions by demonstrating the spatial and temporal trends in modelled budburst dates. Spatial trends demonstrate that the majority of Australian wine regions have the median modelled budburst date during September; however, this varies (ranging between August and November), depending on geographical locations. A temporal analysis showed that modelled budburst dates have been progressively occurring earlier in the year for most wine regions over the 1910–2019 study period and highlighted significant interannual variability associated with large-scale climate drivers, the Indian Ocean Dipole (IOD) and Southern Annular Mode (SAM).

The research presented here may assist in developing management practices to minimise the temperature-related vulnerability of wine regions both in the short and long term. For example, climate driver forecasts are made up to six months in advance by the Australian Bureau of Meteorology (BoM) and other organisations, which could provide lead time in early or delayed budburst. However, it is noted that this should be considered with regard to the limitations linked to the methodologies discussed above, alongside additional future research opportunities.

In terms of long-term planning for climate change, the temporal trends in budburst timing noted here are particularly important. It is projected that the surface temperature trends will be accelerated in coming decades, and at the same time, large-scale climate drivers may increase amplitude and frequency. Collectively, this may cause future changes in budburst timing to be more dramatic. This may also disrupt the subsequent stages of the phenological cycle and place wine grapes at greater risk from frost damage as budburst shifts earlier. Therefore, this information is crucial to prepare robust adaptation plans and identify future opportunities for the Australian wine industry.

Data Availability

The authors declare that the data used to support the findings of this study are included and referenced in the manuscript.

Disclosure

An earlier version of this work was presented as a poster at the Australian Wine Industry Technical Conference and Trade Exhibition (2022).

Conflicts of Interest

The authors declare that they have no conflicts of interest.

Authors' Contributions

The authors have contributed significantly to the manuscript.

Supplementary Materials

Supplementary Table 1: Modelled budburst date Mann–Kendall results for individual wine regions (1910–2019. Supplementary Table 2: *t*-test results (p value) for climate drivers at individual wine regions. Supplementary Table 3: Change in modelled budburst dates between positive and negative phases of climate drivers. (*Supplementary Materials*)

References

[1] G. McIntyre, L. Lider, and N. Ferrari, "The chronological classification of grapevine phenology," *American Journal of Enology and Viticulture*, vol. 33, no. 2, pp. 80–85, 1982.

[2] J. Gladstones, *Viticulture and Environment*, Winetitles, Australia, 1992.

[3] A. Winkler, J. Cook, W. Kliewer, and L. Lider, *General Viticulture. Berkeley*, University of California Press, Oakland, CA, USA, 1974.

[4] A. Alikadic, I. Pertot, E. Eccel et al., "The impact of climate change on grapevine phenology and the influence of altitude: a regional study," *Agricultural and Forest Meteorology*, vol. 271, pp. 73–82, 2019.

[5] A. Caffarra and E. Eccel, "Projecting the impacts of climate change on the phenology of grapevine in a mountain area," *Australian Journal of Grape and Wine Research*, vol. 17, no. 1, pp. 52–61, 2011.

[6] A. Hall, A. J. Mathews, and B. P. Holzapfel, "Potential effect of atmospheric warming on grapevine phenology and post-harvest heat accumulation across a range of climates," *International Journal of Biometeorology*, vol. 60, no. 9, pp. 1405–1422, 2016.

[7] A. C. Malheiro, R. Campos, H. Fraga, J. Eiras-Dias, J. Silvestre, and J. A. Santos, "Winegrape phenology and temperature relationships in the lisbon wine region, Portugal," *OENO One*, vol. 47, no. 4, pp. 287–299, 2013.

[8] L. Webb, P. Whetton, and E. Barlow, "Modelled impact of future climate change on the phenology of winegrapes in Australia," *Australian Journal of Grape and Wine Research*, vol. 13, no. 3, pp. 165–175, 2007.

[9] G. Jones and R. E. Davis, "Climate influences on grapevine phenology, grape composition, and wine production and quality for Bordeaus, France," *American Journal of Enology and Viticulture*, vol. 51, pp. 249–261, 2000.

[10] L. B. Webb, I. Watterson, J. Bhend, P. H. Whetton, and E. W. R. Barlow, "Global climate analogues for winegrowing regions in future periods: projections of temperature and precipitation," *Australian Journal of Grape and Wine Research*, vol. 19, no. 3, pp. 331–341, 2013.

[11] AWRI, *Frost Management in Vineyards, Fact Sheet Viticulture*, Australian Wine Research Institute, Urrbrae, Australia, 2017, https://www.awri.com.au/wp-content/uploads/2017/10/Frost-fact-sheet.pdf.

[12] D. L. Gobbett, U. Nidumolu, and S. Crimp, "Modelling frost generates insights for managing risk of minimum temperature extremes," *Weather and Climate Extremes*, vol. 27, Article ID 100176, 2020.
[13] W. Cameron, P. R. Petrie, E. Barlow, C. Patrick, K. Howell, and S. Fuentes, "Advancement of grape maturity: comparison between contrasting cultivars and regions," *Australian Journal of Grape and Wine Research*, vol. 26, no. 1, pp. 53–67, 2020.
[14] C. Jarvis, R. Darbyshire, I. Goodwin, E. Barlow, and R. Eckard, "Advancement of winegrape maturity continuing for winegrowing regions in Australia with variable evidence of compression of the harvest period," *Australian Journal of Grape and Wine Research*, vol. 25, no. 1, pp. 101–108, 2019.
[15] S. Reis, H. Fraga, C. Carlos et al., "Grapevine phenology in four Portuguese wine regions: modeling and predictions," *Applied Sciences*, vol. 10, no. 11, p. 3708, 2020.
[16] L. B. Webb, P. H. Whetton, and E. W. R. Barlow, "Observed trends in winegrape maturity in Australia," *Global Change Biology*, vol. 17, no. 8, pp. 2707–2719, 2011.
[17] A. Hall and G. V. Jones, "Spatial analysis of climate in winegrape-growing regions in Australia," *Australian Journal of Grape and Wine Research*, vol. 16, no. 3, pp. 389–404, 2010.
[18] L. Hannah, P. R. Roehrdanz, M. Ikegami et al., "Climate change, wine, and conservation," *Proceedings of the National Academy of Sciences of the USA*, vol. 110, no. 17, pp. 6907–6912, 2013.
[19] G. V. Jones, *Climate Change in the Western united states Grape Growing Regions*, International Society for Horticultural Science (ISHS), Leuven, Belgium, 2005.
[20] C. Liles and D. C. Verdon-Kidd, "Refining the growing season temperature parameter for use in winegrape suitability analysis," *Australian Journal of Grape and Wine Research*, vol. 26, no. 4, pp. 343–357, 2020.
[21] D. C. Godwin, R. J. G. White, K. J. Sommer, R. R. Walker, I. Goodwin, and P. R. Clingeleffer, "VineLOGIC - a model of grapevine growth development and water use," *Managing water: Mildura Arts Centre, Mildura, Victoria*, pp. 45–50, Australian Society of Viticulture and Oenology Inc, Adelaide, Australia, 2002.
[22] C. Jarvis, *Using EL Stages and Growing Degree Day Data to Aid Growing Season Planning*, 86 pages, nDPI, Pisa, Italy, 2019.
[23] M. W. Moncur, K. Rattigan, D. H. Mackenzie, and G. N. Mc Intyre, "Base temperatures for budbreak and leaf appearance of grapevines," *American Journal of Enology and Viticulture*, vol. 40, no. 1, pp. 21–26, 1989.
[24] B. B. Fitzharris and W. Enducher, "Climatic conditions for wine grape growing: central Europe and New Zealand," *New Zealand Geographer*, vol. 52, no. 1, pp. 1–11, 1996.
[25] E. Peyer and W. Koblet, "Der Einfluss der Temperatur und der Sonnenstunden auf den Blützeitpunkt der Reben," *Schweizerische Zeitschrift für Obst- und Weinbau*, vol. 10, pp. 250–255, 1966.
[26] R. Pouget, *The Vine Varieties of French AOC Vineyards: History and Possibilities of Development [appellation of Controlled Origin]*, Bulletin de l'OIV, France, 1988.
[27] I. García de Cortázar-Atauri, N. Brisson, and J. P. Gaudillere, "Performance of several models for predicting budburst date of grapevine (Vitis vinifera L.)," *International Journal of Biometeorology*, vol. 53, no. 4, pp. 317–326, 2009.
[28] J. Gladstones, *Wine, Terroir and Climate Change*, Wakefield Press, Adelaide, Australia, 2011.
[29] C. Jarvis, R. Darbyshire, R. Eckard, I. Goodwin, and E. Barlow, "Influence of El niño-southern oscillation and the Indian Ocean Dipole on winegrape maturity in Australia," *Agricultural and Forest Meteorology*, vol. 248, pp. 502–510, 2018.
[30] J. Lopes, J. Eiras-Dias, F. Abreu, P. Climaco, J. Cunha, and J. Silvestre, "Thermal requirements, duration and precocity of phenological stages of grapevine cultivars of the Portuguese collection," *Ciência e Técnica Vitivinícola*, vol. 23, no. 1, pp. 61–71, 2008.
[31] D. Molitor, J. Junk, D. Evers, L. Hoffmann, and M. Beyer, "A high-resolution cumulative degree day-based model to simulate phenological development of grapevine," *American Journal of Enology and Viticulture*, vol. 65, no. 1, pp. 72–80, 2014.
[32] B. G. Coombe and P. Dry, *Viticulture*, Winetitles, Adelaide, Australia, 2004.
[33] M. Webb, A. Pirie, D. Kidd, and B. Minasny, "Spatial analysis of frost risk to determine viticulture suitability in Tasmania, Australia," *Australian Journal of Grape and Wine Research*, vol. 24, no. 2, pp. 219–233, 2018.
[34] CSIRO and Bureau of Meteorology, *State of the Climate*, 2018.
[35] D. A. Jones and B. C. Trewin, "On the relationships between the El Niño–Southern Oscillation and Australian land surface temperature," *International Journal of Climatology*, vol. 20, no. 7, pp. 697–719, 2000.
[36] D. C. Verdon and S. W. Franks, "Indian Ocean sea surface temperature variability and winter rainfall: eastern Australia," *Water Resources Research*, vol. 41, no. 9, 2005.
[37] M. Barrucand, M. Zitto, R. Piotrkowski, and P. Canziani, "Historical southern annular mode index derived from 20th century reanalysis and era 20 c: an overview annular modes: the sam index," in *Proceedings of the 5th International Conference on Reanalysis (ICR5) 2017*, Rome, Italy, November 2017.
[38] N. P. Gillett, T. D. Kell, and P. D. Jones, "Regional climate impacts of the southern annular mode," *Geophysical Research Letters*, vol. 33, no. 23, p. L23704, 2006.
[39] C. Jarvis, E. Barlow, R. Darbyshire, R. Eckard, and I. Goodwin, "Relationship between viticultural climatic indices and grape maturity in Australia," *International Journal of Biometeorology*, vol. 61, no. 10, pp. 1849–1862, 2017.
[40] C. Jarvis, R. Darbyshire, I. Goodwin, E. Barlow, and R. Eckard, "Spatial variation in springtime temperature index values during ENSO and IOD events shows non-equivalent phase response for viticultural regions in Australia," *Agricultural and Forest Meteorology*, vol. 250-251, pp. 217–225, 2018.
[41] P. Whetton, M. Ekstrom, and C. Gerbing, *Climate Change in Australia Information for Australia's Natural Resource Management Regions: Technical Report*, CSIRO and Bureau of Meteorology, Adelaide, Australia, 2015.
[42] K. Anderson and N. R. Aryal, *Which Winegrape Varieties Are Grown where? A Global Empirical Picture*, University of Adelaide Press, Adelaide, Australia, 2020.
[43] Geoscience Australia, *Digital Elevation Model (DEM) of Australia Derived from LiDAR 5 Metre Grid*, Geoscience Australia, Symonston, Australia, 2015.
[44] Wine Australia, *National Vinatge Report*, Wine Australia, Australia, 2021.
[45] N. A. Rayner, D. E. Parker, E. Horton et al., "Global analyses of sea surface temperature, sea ice, and night marine air temperature since the late nineteenth century," *Journal of Geophysical Research*, vol. 108, no. D14, p. 4407, 2003.
[46] B. Huang, P. W. Thorne, V. F. Banzon et al., "NOAA extended reconstructed sea surface temperature (ERSST), version 5," *NOAA National Centers for Environmental Information*, vol. 30, pp. 8179–8205, 2017.

[47] S. Dhame, A. S. Taschetto, A. Santoso, and K. J. Meissner, "Indian Ocean warming modulates global atmospheric circulation trends," *Climate Dynamics*, vol. 55, no. 7-8, pp. 2053–2073, 2020.

[48] F. Chiew and L. Siriwardena, *Trend*, CRC for Catchment Hydrology, 2005.

[49] M. M. Hussain and I. Mahmud, "pyMannKendall: a python package for non parametric Mann Kendall family of trend tests," *Journal of Open Source Software*, vol. 4, no. 39, p. 1556, 2019.

[50] E. Jones, T. Oliphant, and P. Peterson, *SciPy: Open Source Scientific Tools for Python*, 2001.

[51] M. L. Waskom, "seaborn: statistical data visualization," *Journal of Open Source Software*, vol. 6, no. 60, p. 3021, 2021.

[52] IPCC, *Climate Change 2021: The Physical Science Basis. Contribution of Working Group I to the Sixth Assessment Report of the Intergovernmental Panel on Climate Change*, V. Masson-Delmotte, P. Zhai, A. Pirani et al., Eds., Cambridge University Press, Cambridge, UK, 2021.

[53] C. T. Y. Chung and S. B. Power, "The non-linear impact of El Niño, La Niña and the Southern Oscillation on seasonal and regional Australian precipitation," *Journal of Southern Hemisphere Earth Systems Science*, vol. 67, no. 1, pp. 25–45, 2017.

[54] W. Cai, T. Cowan, and M. Raupach, "Positive Indian Ocean Dipole events precondition southeast Australia bushfires," *Geophysical Research Letters*, vol. 36, no. 19, p. L19710, 2009.

[55] S.-K. Min, W. Cai, and P. Whetton, "Influence of climate variability on seasonal extremes over Australia," *Journal of Geophysical Research: Atmospheres*, vol. 118, no. 2, pp. 643–654, 2013.

[56] N. Saji, T. Ambrizzi, and S. E. T. Ferraz, "Indian Ocean Dipole mode events and austral surface air temperature anomalies," *Dynamics of Atmospheres and Oceans*, vol. 39, no. 1-2, pp. 87–101, 2005.

[57] P. R. Petrie and P. R. Clingeleffer, "Effects of temperature and light (before and after budburst) on inflorescence morphology and flower number of Chardonnay grapevines (Vitis vinifera L.)," *Australian Journal of Grape and Wine Research*, vol. 11, no. 1, pp. 59–65, 2005.

[58] Bureau of Meteorology, *About Frost*, http://www.bom.gov.au/climate/map/frost/what-is-frost.shtml, 2014.